

# Effect of ethylene carbonate concentration on structural and electrical properties of PEO–PMMA polymer blends

Poonam Sharma · D. K. Kanchan · Nirali Gondaliya

Received: 18 May 2012 / Revised: 1 August 2012 / Accepted: 19 August 2012 / Published online: 6 September 2012  
© Springer-Verlag 2012

**Abstract** Polyethylene oxide–polymethyl methacrylate (PEO–PMMA) polymer blend electrolyte system complexed with silver salt having different ethylene carbonate (EC) concentrations was prepared using solution cast technique. Complex formation and change in structural and microstructural properties have been studied by X-ray diffraction, Fourier transform infrared, and scanning electron microscopy analysis. The thermal properties of polymer films have been examined by the differential scanning calorimetry technique. Addition of plasticizer is observed to lower melting temperature. Electrical response of polymer films has been measured as a function of EC concentration and temperature using complex impedance spectroscopy. Complex impedance data are used to analyze the conductivity, permittivity, and modulus formalism to understand the conduction mechanism. The temperature dependence of electrical conductivity of polymer electrolytes shows a sudden rise at the melting temperature of PEO.

**Keywords** PEO–PMMA polymer blend · XRD · SEM · Plasticizer · Relaxation

## Introduction

Optimization of the electrochemical properties of solid polymer electrolytes is an area of intense interest. Many groups

have attempted over the years to enhance the electrochemical properties of polymer electrolytes with the addition of plasticizer, dispersal of nanofillers, addition of ionic liquid, blending of polymers, etc. [1–8]. Each of these modified systems has its own strengths and weaknesses. For instance, polymer blending provides a strategic route to improve the performance of the electrolyte over each individual polymer. In addition to this, it also allows realization of novel materials which possess enhanced performance over the parent polymer. Consequently, in the last decades, many polymer blends, e.g., PVdF–PEMA, PEO–PMMA, PVC–PMMA, PMMA–PVdF (where PVdF—polyvinylidene fluoride, PEMA—polyethyl methacrylate, PEO—polyethylene oxide, PMMA—polymethyl methacrylate, PVC—polyvinyl chloride), etc., were developed [8–12]. Out of the so far reported polymer blends, PEO–PMMA is one of the most studied polymer blends, and among the various studies carried out in this system, considered significant are (1) Li-ion conduction in PEO–PMMA polymer blends [8], (2) dynamics of PEO in PEO–PMMA polymer blends [13], and (3) application of PEO–PMMA polymer electrolyte as fuel cell [14]. Blending of PEO with PMMA inhibits the crystallization of PEO [12]. As a result of this, an enhancement in conductivity is expected because of the increased amorphous regions of the polymer host as conduction is generally taking place in the amorphous regions of PEO.

It is well known that plasticization of polymers is an important approach to increase the ionic conductivity of electrolytes [2–5]. Plasticizers are small organic molecules which embed themselves between the polymer chains and increase the spacing and free volume resulting in improvement of the conductivity of polymer electrolytes by dissociating ion aggregates [3, 4]. Basically, plasticizers penetrate easily in the host polymer matrix and cause an interaction between polymer chains. This, in turn, reduces the cohesive forces between polymer chains and increases the segmental chain mobility.

P. Sharma · D. K. Kanchan (✉) · N. Gondaliya  
Solid State Ionics & Glass Research Laboratory, Department of  
Physics, Faculty of Science, The Maharaja Sayajirao University of  
Baroda,  
Vadodara, Gujarat 390002, India  
e-mail: d\_k\_kanchan@yahoo.com

N. Gondaliya  
Department of Engineering Physics, SVMIT,  
Bharuch, Gujarat, India

In spite of the reported work on PEO–PMMA polymer blends [8, 12–15], nevertheless, the structural and electrical properties of the silver ion conducting PEO–PMMA polymer system have not been undertaken earlier and have attracted attention to study the effect of the plasticizer, ethylene carbonate (EC), in this system.

## Experimental description

### Starting materials

Commercially available chemicals of PEO ( $M_w=3 \times 10^5$ , Alfa Aesar), PMMA ( $M_w=3.5 \times 10^5$ , Alfa Aesar), silver nitrate ( $\text{AgNO}_3$ ), and EC (Aldrich) were employed as starting materials. The compositions of the polymer films are given in Table 1. All the samples were prepared by the solution cast method.

### Sample preparation

PEO and PMMA were dissolved in acetonitrile separately and stirred by using a magnetic stirrer. The stirring of the PMMA solution was carried out at 323 K for 24 h to dissolve PMMA in acetonitrile. PEO and  $\text{AgNO}_3$  were mixed and stirred for 4–5 h at room temperature. Both solutions were mixed along with the desired amount of plasticizer. The obtained mixture was again stirred at room temperature for another 10 h for homogenous mixing. Finally, the solution was poured into a Teflon Petri dish, and the solvent was left to evaporate slowly at ambient temperature. The resulting films were kept in an oven at 313 K for 2 days to ensure the removal of solvent traces. The dried films were peeled off from the Petri dish and then were stored in dark desiccators to prevent any contamination from moisture or effect from light.

### Characterization

The X-ray diffraction (XRD) measurement was carried out using monochromatic  $\text{Cu-K}\alpha$  radiation ( $=1.5418 \text{ \AA}$ ) in an X-ray diffractometer (Bruker NSZ, model D8) in the range of  $10\text{--}70^\circ$  at a scan rate of  $2^\circ/\text{min}$ . The surface morphology

of the plasticized polymer complexes was investigated using a scanning electron microscope (SEM) (JOEL JSM-6380LV) at 20 kV. The polymer films were gold-coated in vacuum by an electron beam gold palladium source (80 % Au, 20 % Pd) by JEOL coater (Model JFC-1600) to make them conducting and mounted onto circular aluminum stubs by using double-sided sticky tapes.

Differential scanning calorimetry (DSC) of the prepared polymer films was carried out using SII EXSTAR-6000 equipment in the range from room temperature to 363 K with a heating rate of 10 K/min in nitrogen atmosphere. The polymer samples of about 2–3 mg were encapsulated in aluminum pans. Fourier transform infrared (FT-IR) spectra of the prepared samples were recorded in the wave number range of  $4,000\text{--}400 \text{ cm}^{-1}$  using single beam FT-IR 4100 JASCO model by directly mounting in the sample holder in a transmission mode.

### Electrical measurements

Complex impedance spectroscopy was employed for electrical measurements using the impedance gain/phase analyzer (SOLARTRON 1260) interfaced to a computer in the frequency range of 100 Hz to 1 MHz at various temperatures ranging between 303 and 373 K. For the impedance measurements, the polymer electrolyte films were sandwiched between two silver electrodes of 1 cm radius under spring pressure in a temperature-controlled furnace. The obtained impedance plots were fitted using Zview2 program (developed by Solartron Analytical).

## Results and discussion

### XRD

In the present study, the XRD patterns of the plasticized polymer films are recorded along with pure PEO and PMMA to correlate the structure of polymer complexes. Pure PMMA exhibits a broad hump (inset of Fig. 1a) while the characteristic crystalline peaks of pure PEO are observed at  $19.3^\circ$  and  $23.7^\circ$  (Fig. 1a). In the prepared polymer films, the intensity of PEO peaks is observed to be less, and in

**Table 1** Plasticized polymer blend compositions

Sample name	Weight percentage of EC	Weight percentage of PEO	Weight percentage of PMMA	Weight percentage of $\text{AgNO}_3$
EC-5	5	50	50	5
EC-7	7	50	50	5
EC-10	10	50	50	5
EC-12	12	50	50	5
EC-15	15	50	50	5

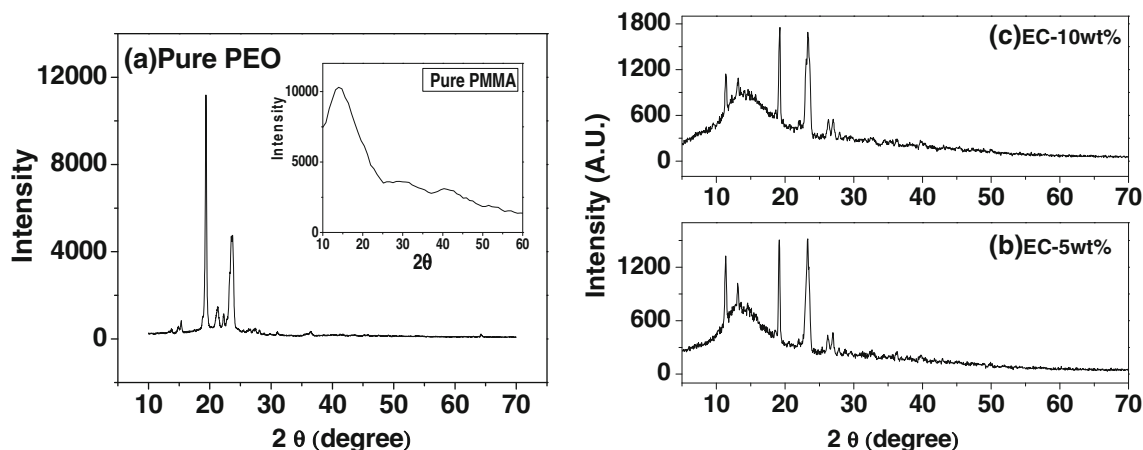


**Fig. 1** XRD plots for **a** pure PEO and *inset* shows pure PMMA; **b** PEO (50)–PMMA (50)–AgNO<sub>3</sub> (5)–EC (5); **c** PEO (50)–PMMA (50)–AgNO<sub>3</sub> (5)–EC (10) plasticized polymer electrolytes

addition to this, two new peaks at 11° and 13° are observed only in EC-5 wt% and EC-10 wt% polymer films. Less intensity of XRD diffraction peaks of PEO in polymer films indicates the presence of a semi-crystalline phase of PEO and reduction in degree of crystallinity. These observations may be due to the plasticization effect of EC; however, the blending effect of PEO–PMMA cannot be ignored. With the increase in EC concentration, the relative intensity of X-ray peaks is observed to decrease which is an indication of reduction of crystalline phase in polymer complexes. However, for EC-7 wt%, the intensity of XRD peaks is observed to be higher than other polymer films. The absence of AgNO<sub>3</sub> peaks [16] and the above discussion suggest complexation of AgNO<sub>3</sub> in the polymer matrix as well as interactions between the plasticizer and polymers.

## SEM

SEM spectroscopy provides a powerful tool for monitoring surface morphology. Figure 2a–c shows the SEM micrographs of the plasticized polymer complexes with different plasticizer concentrations. Figure 2a represents a SEM micrograph of the EC-5 wt% polymer blend which shows some smooth areas, indicating the homogeneity among various constituents of the polymer matrix. Increasing EC concentration as plasticizer (Fig. 2b), a substantial change in the morphological feature (spherulite texture) of the composite starts appearing. The boundary between the spherulites is an indication of the existence of an amorphous phase. At EC-10 wt%, with decrease in size, the spherulites become distinctive which in turn increases the boundary regions. At EC-15 wt%, the polymer blend film exhibits good distribution of amorphous and crystalline regions inside the polymer complex (Fig. 2c).

## DSC

The DSC plots of plasticized polymer blends show a sharp endothermic peak indicating transition from a semi-crystalline

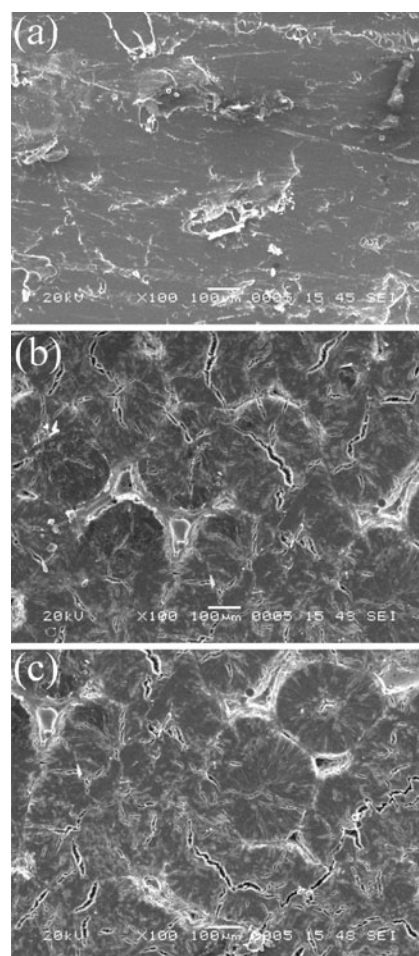


**Fig. 2** SEM micrographs of PEO–PMMA–AgNO<sub>3</sub>: **a** EC-5 wt%, **b** EC-10 wt%, and **c** EC-15 wt% polymer blend films

phase to an amorphous phase, i.e., melting temperature ( $T_m$ ) of PEO. Table 2 lists  $T_m$ , percentage of degree of crystallinity, and FWHM values at different EC concentrations in plasticized polymer complexes. The increase in EC concentration possibly reduces the internal viscosity of the polymer films; in other words, it interrupts polymer–polymer interaction by occupying the inter- and intra-chain free volume which reduces the crystalline fraction of the polymer system, leading to an enhancement in the flexibility of the polymer chains [17]. The percentage of degree of crystallinity of the polymer films has been calculated using the relation:

$$X_c\% = (\Delta H / \Delta H_0) \times 100 \quad (1)$$

where  $\Delta H_0$  is the enthalpy of melting of polymer films, and  $\Delta H$  (213.7 J/g) is the enthalpy of melting of 100 % crystalline PEO [18]. The FWHM value or broadness of the melting peak increases with EC concentration, which indicates an increase in amorphous phases with EC concentration. These observed variations in  $T_m$ , percentage degree of crystallinity, and FWHM values suggest the complexation of EC with an increase in amorphous phase in the host polymer blend.

#### FT-IR

Infrared spectroscopy measures the vibrational energy levels in the region of different molecules. The IR spectra of materials vary according to their compositions and show the occurrence of the complexation and interaction between various constituents. Hirankumar et al. [16] reported characteristic peak of pure  $\text{AgNO}_3$  at 1,800 and 1,430  $\text{cm}^{-1}$ . The IR spectra of pure PEO, PMMA, and plasticized polymer complexes are given in panels a and b of Fig. 3 in various wave number ranges. The broad band observed in the wave number range of 2,950–2,700  $\text{cm}^{-1}$  (Fig. 3b) in pure PEO is attributed to the symmetric and asymmetric C–H stretching modes of the  $\text{CH}_2$  group [19]. In pure PEO, scissoring, wagging, twisting, and rocking modes of  $\text{CH}_2$  are observed at 1,461, 1,338, 1,276, and 844  $\text{cm}^{-1}$ , respectively, while C–O–C bending at 537  $\text{cm}^{-1}$  is observed [19–22]. In pure PMMA, the peaks at 1,721, 1,433, and 1,137  $\text{cm}^{-1}$  are

assigned to C=O,  $-\text{OCH}_3$  deformation, and C–O stretching vibrations, respectively [11, 23–26]. The band at 986  $\text{cm}^{-1}$  is attributed to the symmetrical stretching of the C–O bond in the C–O–C linkage of PMMA [26]. The frequency at 1,275  $\text{cm}^{-1}$  is assigned to asymmetric  $\text{CH}_2$  transformation of PMMA.

In the present investigated system, the characteristic peak of  $\text{AgNO}_3$  at 1,800  $\text{cm}^{-1}$  broadens, indicating complexation of salt with the polymer blend. In the prepared polymer films (Fig. 3b), the stretching frequency at 1,721  $\text{cm}^{-1}$  corresponding to C=O of pure PMMA is broadened and shifted to 1,709–1,746  $\text{cm}^{-1}$ , which indicates complex formation [25]. The triplet peak of C–O–C stretching of PEO is absent and  $\text{CH}_2$  rocking vibration of pure PEO is observed to shift to 839  $\text{cm}^{-1}$ . The stretching vibration of the methoxy group and the wagging mode of  $\text{CH}_2$  of pure PMMA and PEO, respectively, are absent in polymer complexes. In addition to this, some small new peaks at 1,964  $\text{cm}^{-1}$  and

**Table 2** Thermal properties of PEO–PMMA– $\text{AgNO}_3$ –EC polymer electrolyte system

Sample	Melting temperature, $T_m$ (K)	Degree of crystallinity (%)	FWHM of $T_m$ peak
EC-5	335.4	20.3	3.76
EC-7	335.8	30.1	3.43
EC-10	333.6	24.8	4.15
EC-12	332.5	23.8	5.62
EC-15	330.59	13	6.96

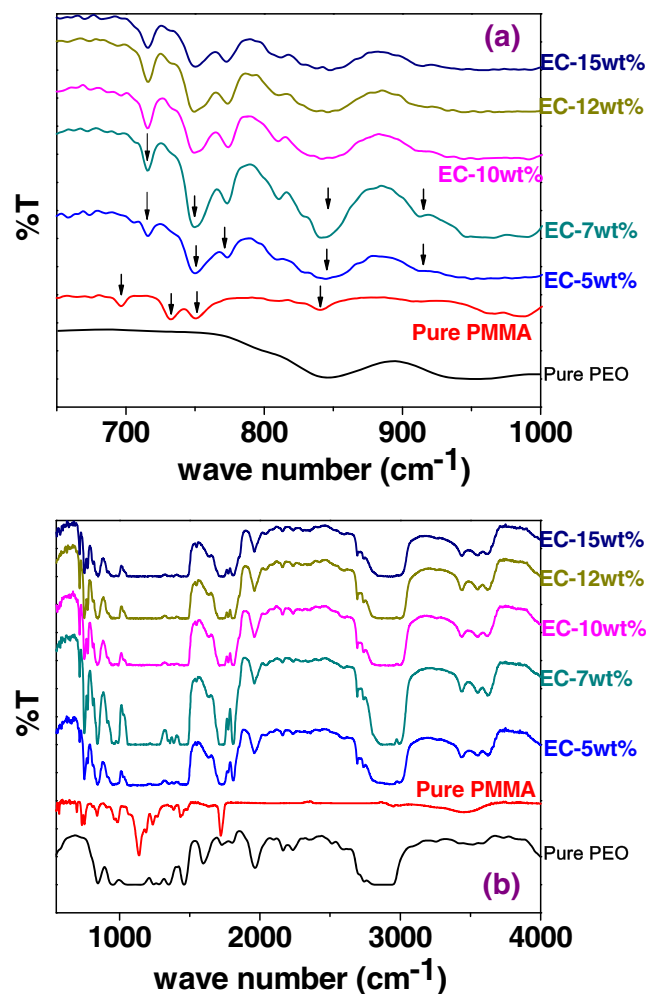


**Fig. 3** IR spectra of pure PEO, pure PMMA, and different concentrations of EC in PEO–PMMA– $\text{AgNO}_3$  polymer blends in the wave number range of **a** 600–1,000  $\text{cm}^{-1}$  and **b** 600–4,000  $\text{cm}^{-1}$

in the range of 2,690–3,630  $\text{cm}^{-1}$  are observed. Also, the bending mode of EC at 903  $\text{cm}^{-1}$  [27] shifts to 912  $\text{cm}^{-1}$  in polymer complexes indicating the interaction of salt and EC. In the FT-IR spectra, the disappearance and change in position of PEO and PMMA vibrational bands along with some new peaks confirm the complexation among various constituents of PEO–PMMA polymer electrolytes.

Conductivity

The ionic conductivity of the polymer films,  $\sigma$ , was calculated using the relation:

$$\sigma = (t/A)(1/R_b) \tag{2}$$

where  $t$  is the thickness of the film,  $A$  is the contact area of the polymer film, and  $R_b$  is the bulk resistance of the polymer film.  $R_b$  values were determined from the intercept of a high frequency semicircle at the  $x$ -axis. As shown in Fig. 4, conductivity initially drops as EC content increases from 5 to 7 wt%, and thereafter, it increases nonlinearly. In the polymer film with EC-7 wt%, the increase in the degree crystallinity as evident from XRD and DSC studies may be responsible for the drop in conductivity. After 7 wt% of EC concentration, the increase in conductivity with plasticizer concentration in polymer complexes may be due to a high value of dielectric constant of EC that effectively reduces the inter-ion Coulomb interactions [28], and more number of  $\text{Ag}^+$  ions contributed to the conductivity of the complexes. Lastly, the addition of plasticizer in the polymer matrix also facilitates to decrease the ion pairing which produces a great number of charge carriers for ionic transport. Furthermore, the addition of EC lowers the melting temperature and increases the amorphous phase of the polymer blend, corresponding to conductivity

enhancement. Hence, the increase in conductivity plot may be due to the higher content of the plasticizer due to which more salt has been dissociated which must have favored the enhancement in conductivity. Rhoo et al. [29] have suggested that with higher plasticizer content, opening of the narrow rivulets of the plasticizer-rich phase and large free volume of relatively superior conducting phase has taken place which results in greater ionic transport.

The inset of Fig. 4 shows the temperature dependence of ionic conductivity for EC-5 wt%. Similar behavior of conductivity with different values has been observed for different concentrations. The ionic conductivity of the plasticized polymer complex increases with temperature. The inset shows a sudden and/or sharp rise in conductivity near  $T_m$ . The observed sharp rise around 333 K is due to the softening of PEO polymer near  $T_m$  in the polymer complexes which is reported by several workers in PEO-based polymer electrolyte systems [19, 20]. The viscosity and crystallinity of the polymer system decrease near the melting temperature, and hence, polymer chains become more flexible resulting in an increase in segmental motion leading to a sharp rise in conductivity.

Figure 5 shows the compositional variation of AC conductivity at 323 K. It shows similar result as observed in ionic conductivity variation with EC concentration, i.e., AC conductivity values are higher in the polymer films with EC-5 wt% and EC-15 wt%. Figure 6 represents the temperature dependence of AC conductivity of EC-5 wt% polymer film. AC conductivity is observed to increase with temperature as well as frequency. Below  $T_m$ , AC conductivity shows two dispersion regions, namely, one in the low frequency region and the other in the high frequency region. As temperature approaches  $T_m$ , dispersion in the low frequency region

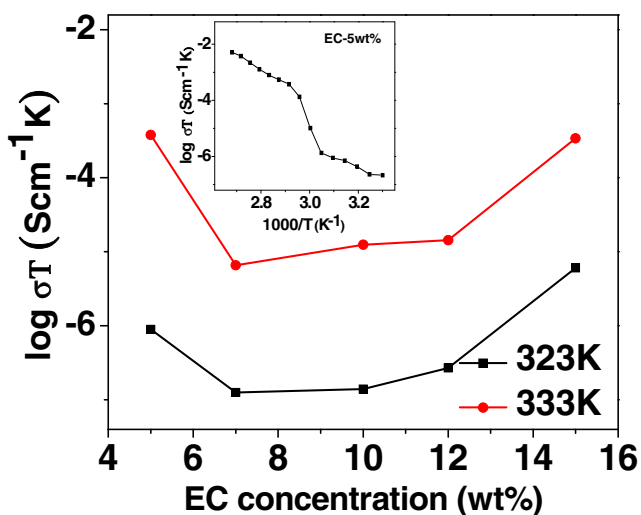


Fig. 4 Compositional variation of ionic conductivity and inset shows the temperature dependence of conductivity for the polymer film of PEO–PMMA–AgNO<sub>3</sub>–EC (5 wt%)

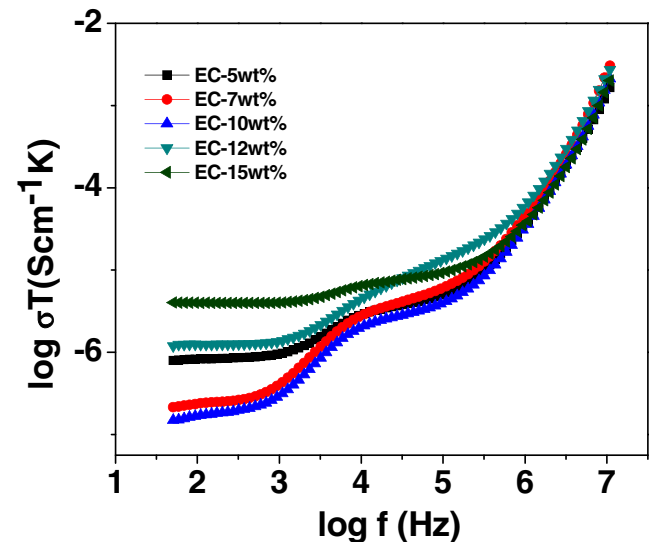
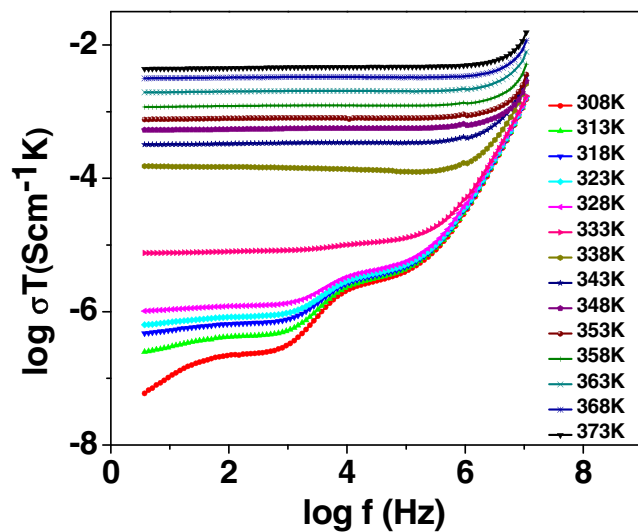


Fig. 5 AC conductivity plot of PEO–PMMA–AgNO<sub>3</sub>–EC polymer electrolytes for different concentrations of EC at 323 K



**Fig. 6** AC conductivity plot for PEO-PMMA-AgNO<sub>3</sub> polymer film with EC (5 wt%) at various temperatures

disappears and only the high frequency dispersion region is observed. At higher temperatures ( $T > T_m$ ), the AC conductivity is frequency independent in the low frequency region. In the high frequency region, AC conductivity shows a dispersion, which shifts to higher frequencies with increase in temperature as observed in Fig. 6. The frequency dispersion effects are present in all the samples. In the high frequency region, mobility of charge carriers, Ag<sup>+</sup>, is high near the relaxation times, and hence, conductivity increases with frequency. This variation of conductivity with frequency has been analyzed using the relation given by Jonscher [30]

$$\sigma(\omega) = \sigma_{DC} + A\omega^s \quad (3)$$

where the symbols have their usual meanings. The above expression is known as the power law of AC behavior because the power law of AC behavior is observed in a wide range of materials and is called as “Jonscher’s universal behavior.”

#### Dielectric studies

The dielectric properties of the polymer electrolyte system can be characterized by frequency-dependent parameters such as complex permittivity ( $\epsilon^*$ ) which is defined as [31]:

$$\epsilon^*(\omega) = \epsilon'(\omega) - j\epsilon''(\omega) = 1/j\omega C_0 Z^* \quad (4)$$

where  $\epsilon'$  and  $\epsilon''$  represent the real and imaginary parts of the dielectric constant,  $\omega$  is the angular frequency,  $C_0$  represents the vacuum capacitance of any configurations of the electrode, and  $Z^*$  is the complex impedance. The dielectric spectra contain contribution from dipolar orientation as well as diffusion of charge carrier. Figure 7 and its inset show the influence of various concentrations of EC at frequency-dependent  $\epsilon'$  and  $\epsilon''$ , respectively, at 323 K. The figure

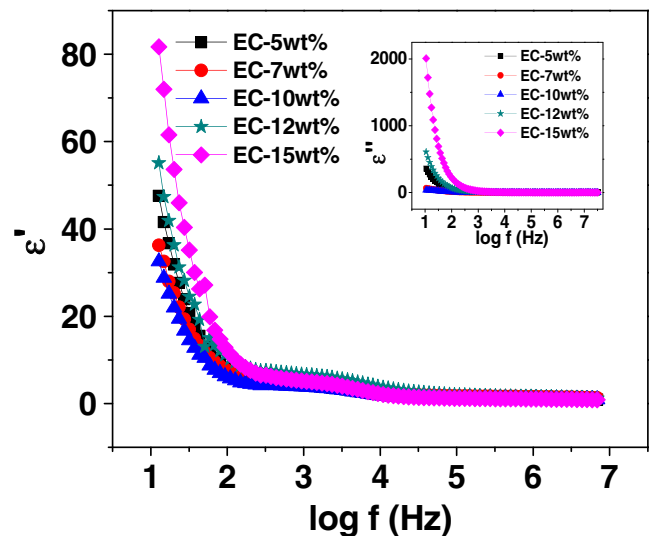


**Fig. 7** Real and imaginary (*inset*) parts of dielectric permittivity,  $\epsilon^*$  plots as a function of frequency for plasticized PEO-PMMA-AgNO<sub>3</sub> polymer electrolytes with different concentrations of EC at 323 K

shows low frequency dispersion being significant and associated with the space polarization effects arising from the electrodes. In the low frequency region, dipoles follow an oscillating electric field and reorient themselves in the field direction [32], whereas at higher frequencies, the periodic reversal of field is quite high so that contribution of the dipoles may not be able to reorient themselves resulting in low or negligible contribution of the charge carriers. Therefore, the real and imaginary parts of the dielectric constant decrease with increasing frequency and reach a constant value. The compositional variation of frequency-dependent dielectric constant (both  $\epsilon'$  and  $\epsilon''$ ) shows a similar trend as observed from conductivity data, i.e., initially, it decreases as EC concentration increases from 5 to 7 wt%, and beyond that concentration, its values increase. This can be understood with the increased number of dipoles and hence decreased relaxation time at a higher concentration of the plasticizer.

Electrical modulus formalism is useful to study the relaxation process in materials [31]. The electrical relaxation process is due to distribution of relaxation times which may be due to inhomogeneity, conducting domain, mixture of phases, etc. The real,  $M'$ , and imaginary,  $M''$ , parts of the electrical modulus are given by:

$$M^* = M' + jM'' = j\omega C_0 Z^* \quad (5)$$

Frequency-dependent  $M''$  and  $M'$  plots of various concentrations of EC in PEO-PMMA-AgNO<sub>3</sub> polymer films are shown in Fig. 8 and its inset, respectively.  $M'$  and  $M''$  show an increasing trend with frequency at a particular temperature indicating the bulk effect. The lower or negligible values of  $M'$  and  $M''$  at lower frequencies indicate that the electrode polarization phenomenon makes a small

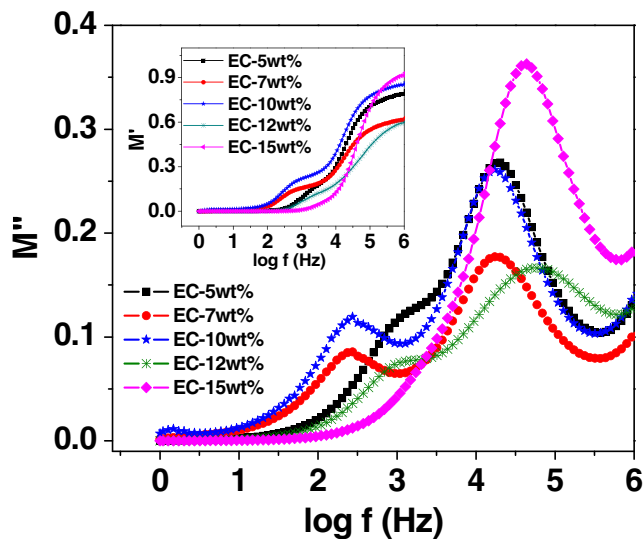


**Fig. 8** Frequency-dependent plot of real part of modulus  $M'$  (inset) and imaginary part of modulus  $M''$  for plasticized PEO–PMMA–AgNO<sub>3</sub> polymer electrolytes for different concentrations of EC at 323 K

contribution to the electrical modulus. Below  $T_m$ ,  $M'$  plot (inset of Fig. 9) shows two dispersion regions which turn into a single one as temperature approaches  $T_m$ . Similarly, below  $T_m$ , the frequency-dependent  $M''$  spectra (Fig. 9) show two peak maxima, and as temperature approaches  $T_m$ , the first peak in the low frequency region disappears and the single relaxation peak in the mid-frequency region remains. These double relaxation features at temperatures  $T < T_m$  are also in agreement with AC conductivity behavior. This behavior can be explained as at higher temperatures, i.e.,  $T > T_m$ , the semi-crystalline regions of PEO melt; in other words, the system becomes amorphous which results

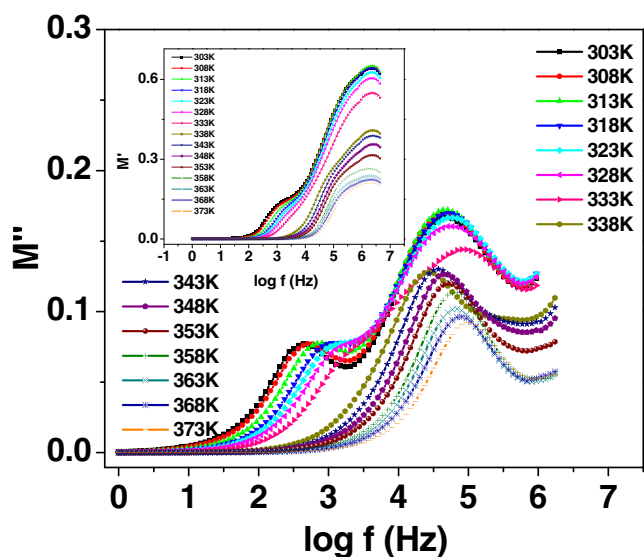


**Fig. 9** Frequency-dependent  $M''$  plot of PEO–PMMA–AgNO<sub>3</sub>–EC (12 wt%) at different temperatures

in single dispersion in conductivity or single relaxation in modulus plots. A detailed study regarding this can be found in our earlier report published elsewhere [15]. At  $T > T_m$ , the frequency of  $M''_{max}$  is found to shift systematically towards the higher frequency side with increase in temperature. Similar features in the modulus spectra below and above the  $T_m$  of PEO in mixed electrolytes of MEEP–PEO doped with NaSCN are observed by Subramony and Kulkarni [31]. Scaling of the modulus spectra [33] has been carried out in order to understand the occurrence of dynamical processes in different concentrations at a particular temperature (Fig. 10). The scaled plot of the modulus does not show a single superposable master curve which indicates that the relaxation processes depend on the EC concentration, i.e., compositional dependent.

Relaxation processes occurring inside the ionic materials can be visualized and distinguished by impedance, electric modulus, and dielectric permittivity [34]. The frequency-dependent imaginary part of complex impedance,  $Z''$ , modulus,  $M''$ , and dielectric permittivity,  $\epsilon''$ , for EC-5 wt% polymer electrolyte are plotted (Fig. 11a–c). The absence or presence of a peak in the imaginary impedance versus the frequency plot can be correlated to space charge effects and nonlocalized conductivity. The  $M''$  plot is very useful when the relaxation behavior is presumed to be due to the motion of ions as in modulus analysis, and the electrode effects occurring at lower frequencies are suppressed. Also, the maxima of  $Z''$  and  $M''$  do not occur at the same frequency, where the  $Z''$  spectrum broadened on the low frequency side while the  $M''$  spectrum broadened on the high frequency side, indicating distribution of relaxation times, i.e., non-Debye nature of polymer films. Dielectric relaxation is a result of the reorientation process of dipoles in the polymer chains, which show a peak in the  $\epsilon''$  spectra. For electrolytes

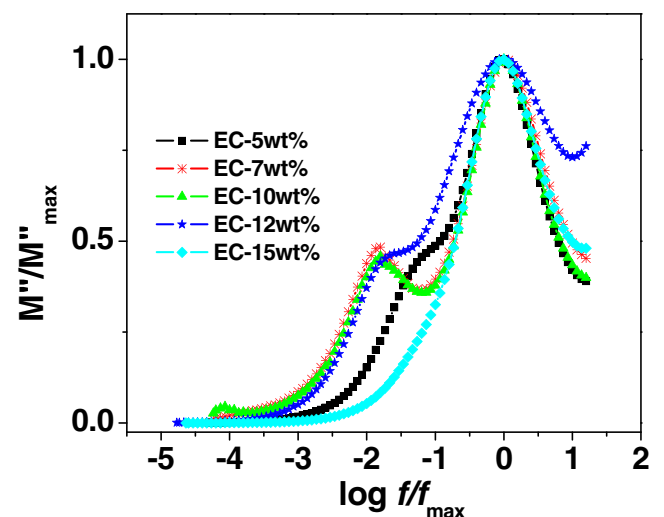


**Fig. 10** Scaled  $M''$  spectra for plasticized PEO–PMMA–AgNO<sub>3</sub> polymer electrolytes with different concentrations of EC at 323 K

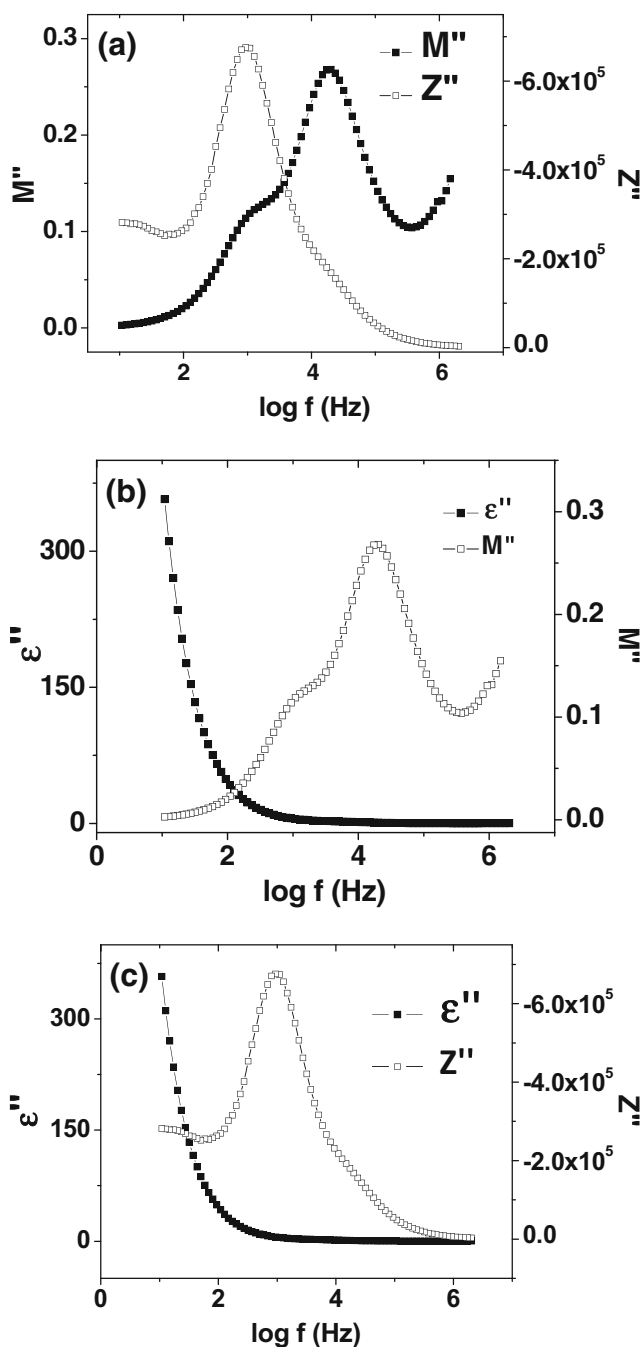


**Fig. 11** **a** Frequency-dependent plot of  $Z''$  and  $M''$  for PEO-PMMA-AgNO<sub>3</sub>-EC (5 wt%) plasticized polymer electrolyte at 323 K. **b** Frequency-dependent plot of  $\epsilon''$  and  $M''$  for PEO-PMMA-AgNO<sub>3</sub>-EC (5 wt%) plasticized polymer electrolyte at 323 K. **c** Frequency-dependent plot of  $\epsilon''$  and  $Z''$  for PEO-PMMA-AgNO<sub>3</sub>-EC (5 wt%) plasticized polymer electrolyte at 323 K

with higher ion concentration, the movement of ions from one site to another perturbs the electric potential of the surroundings. In the imaginary part of the modulus spectra, a relaxation peak is observed (for the conductivity processes), whereas no peak is seen in the dielectric spectra, suggesting that ionic and polymer segmental motion is strongly coupled

and hence manifesting as a single peak in the  $M''$  spectra with no corresponding feature in the dielectric spectra.

## Conclusions

The structural and electrical conductivity behavior of PEO-PMMA-AgNO<sub>3</sub>-EC polymer films has been studied. SEM analysis shows a change in surface morphology with EC concentration. Complexation of the polymer complexes has been established by XRD, FT-IR, and DSC analysis. Conductivity isotherm shows an enhancement in conductivity with EC concentration minima at 7 wt%. The temperature dependence of ionic conductivity shows a sharp rise as temperature approaches  $T_m$ , indicating a liquid-like ion transport in a solid polymer matrix above  $T_m$ . AC conductivity of polymer films increases with temperature and frequency. AC conductivity and modulus spectra show two dispersion regions which turn into a single one as temperature approaches  $T_m$ . The scaling of the imaginary part of the modulus spectra indicates compositional dependence of the relaxation process.

**Acknowledgments** PS thankfully acknowledges the financial support by UGC, New Delhi, India for RFSMS fellowship.

## References

- Pradhan DK, Choudhary RNP, Samantaray BK, Karan NK, Katiyar RS (2007) Effect of plasticizer on structural and electrical properties of polymer nanocomposite electrolytes. *Int J Electrochem Sci* 2:861–871
- Pradhan DK, Samantaray BK, Choudhary RNP, Karan NK, Thomas R, Katiyar RS (2011) Effect of plasticizer on structural and electrical properties of nanocomposite solid polymer electrolytes. *Ionics* 17:127–134
- Kumar M, Sekhon SS (2002) Role of plasticizer's dielectric constant on conductivity modification of PEO-NH<sub>4</sub>F polymer electrolytes. *Eur Polym J* 38:1297–1304
- Kumar M, Sekhon SS (2002) Ionic conductance behaviour of plasticized polymer electrolytes containing different plasticizers. *Ionics* 8:223
- Johan MR, Shy OH, Ibrahim S, Yassin SMM, Hui TY (2011) Effects of Al<sub>2</sub>O<sub>3</sub> nanofiller and EC plasticizer on the ionic conductivity enhancement of solid PEO-LiCF<sub>3</sub>SO<sub>3</sub> solid polymer electrolyte. *Solid State Ionics* 196:41–47
- Pandey GP, Agarwal RC, Hashmi S (2011) Performance studies on composite gel polymer electrolytes for rechargeable magnesium battery applications. *J Phys Chem Solids* 72:1408–1413
- Kumar Y, Hashmi S, Pandey GP (2011) Ionic liquid mediated magnesium ion conduction in poly(ethylene oxide) based polymer electrolytes. *Electrochim Acta* 56:3864–3873
- Osman Z, Ansor NM, Chew KW, Kamarulzaman N (2005) Infrared and conductivity studies on blends of PMMA/PEO based polymer electrolytes. *Ionics* 11:431–435
- Sivakumar M, Subadevi R, Rajendran S, Wu HC, Wu NL (2007) Compositional effect of PVdF-PEMA blend gel polymer electrolytes for lithium polymer batteries. *Eur Polym J* 43:4466–4473



10. Ramesh S, Leen KH, Kumatha K, Arof AK (2007) FTIR studies of PVC/PMMA blend based polymer electrolytes. *Spectrochim Acta A* 66:1237–1242
11. Rajendran S, Kannan R, Mahendran O (2001) An electrochemical investigation on PMMA/PVdF blend-based polymer electrolytes. *Mater Lett* 49:172–179
12. Radhakrishnan S, Venkatachalapathy PD (1996) Effect of casting solvent on the crystallization in PEO/PMMA blends. *Polymer* 37:3749–3752
13. Sakai VG, Maranas JK, Peral I, Copley JRD (2008) Dynamics of PEO in blends with PMMA: study of the effect of blend composition via quasi-elastic neutron scattering. *Macromolecules* 41:3701–3710
14. Przulski J, Dabrowska A, Stys S, Wieczorek W (1993) Ambient temperature proton polymeric electrolytes based on poly(ethylene oxide)–poly(methyl methacrylate) blends. *Solid State Ionics* 60:141–146
15. Sharma P, Kanchan DK, Gondaliya N, Pant M, Jayswal MS (2012) Conductivity relaxation in Ag<sup>+</sup> ion conducting PEO–PMMA–PEG polymer blends. *Ionics*. doi:10.1007/s11581-012-0738-4
16. Hirankumar G, Selvasekarapandian S, Bhuvaneshwari MS, Baskaran R, Vijayakumar M (2006) Ag<sup>+</sup> ion transport studies in a polyvinyl alcohol-based polymer electrolyte system. *J Solid State Electrochem* 10:193–197
17. Platzner NAJ (1965) Plasticization and plasticizer processes. *Advances in Chemistry Series*, vol 48. The American Chemical Society, Washington. doi:10.1021/ba-1965-0048, ISBN13: 9780841200494e ISBN: 9780841222281
18. Money BK, Hariharan K (2007) Lithium ion conduction in lithium metaphosphate based systems. *Appl Phys A* 88:647–652
19. Mohan VM, Raja V, Sharma AK, Rao VVRN (2006) Ion transport and battery discharge characteristics of polymer electrolyte based on PEO complexed with NaFeF<sub>4</sub> salt. *Ionics* 12:219–226
20. Ramesh S, Yuen TF, Shen CJ (2008) Conductivity and FTIR studies on PEO–LiX [X: CF<sub>3</sub>SO<sub>3</sub><sup>-</sup>, SO<sub>4</sub><sup>2-</sup>] polymer electrolytes. *Spectrochim Acta A* 69:670–675
21. Noor SAM, Ahmad A, Talib IA, Rahman MYA (2010) Morphology, chemical interaction, and conductivity of a PEO-ENR50 based on solid polymer electrolyte. *Ionics* 16:161–170
22. Frech R, Chintapalli S, Bruce PG, Vincent CA (1999) Crystalline and amorphous phases in the poly(ethylene oxide)–LiCF<sub>3</sub>SO<sub>3</sub> system. *Macromolecules* 32:808–813
23. Deka M, Kumar A (2010) Enhanced ionic conductivity in novel nanocomposite gel polymer electrolyte based on intercalation of PMMA into layered LiV<sub>3</sub>O<sub>8</sub>. *J Solid State Electrochem* 14:1649–1656
24. Chatterjee A (2010) Properties improvement of PMMA using nano TiO<sub>2</sub>. *J Appl Polym Sci* 118:2890–2897
25. Rajendran S, Bama VS, Prabhu MR (2010) Preparation and characterization of PVAc–PMMA-based solid polymer blend electrolytes. *Ionics* 16:283–287
26. Ramesh S, Bing KN (2012) Conductivity, mechanical and thermal studies on poly(methyl methacrylate)-based polymer electrolytes complexed with lithium tetraborate and propylene carbonate. *J Mater Eng Perform* 21:89–94
27. Kalyanasundaram S, Gopalan A, Muniyandi N, Renganathan NG, Saito Y, Kataoka H, Stephan AM, Elizabeth RN (2001) Ionic conductivity, thermal stability and FT-IR studies on plasticized PVC/PMMA blend polymer electrolytes complexed with LiAsF<sub>6</sub> and LiPF<sub>6</sub>. *Ionics* 7:44–52
28. Johan MR, Ting LM (2011) Structural, thermal and electrical properties of nano manganese-composite polymer electrolytes. *Int J Electrochem Sci* 6:4737–4748
29. Rhoo HJ, Kim HT, Park JK, Hwang TS (1997) Ionic conduction in plasticized PVC/PMMA blend polymer electrolytes. *Electrochim Acta* 42:1571–1579
30. Jonscher AK (1977) The ‘universal’ dielectric response. *Nature* 267:673
31. Subramony JA, Kulkarni AR (1994) Conductivity relaxation in phosphazene based polymer electrolytes. *Solid State Ionics* 67:235–239
32. Ibrahim S, Yasin SMM, Nee NM, Ahmad R, Johan MR (2012) Conductivity and dielectric behaviour of PEO-based solid nanocomposite polymer electrolytes. *Solid State Commun* 152:426–434
33. Karmakar A, Ghosh A (2012) Dielectric permittivity and electric modulus of polyethylene oxide (PEO)–LiClO<sub>4</sub> composite electrolytes. *Curr Appl Phys* 12:539–543
34. Sen S, Pramanik P, Choudhary RNP (2006) Impedance spectroscopy study of the nanocrystalline ferroelectric (PbMg)(ZrTi)O<sub>3</sub> system. *Appl Phys A* 82:549–557